17th World Conference on Earthquake Engineering, 17WCEE
Sendai, Japan - September 13th to 18th 2020

EARTHQUAKE-INDUCED LOSS AND COLLAPSE RISK ASSESSMENT OF STEEL SEGMENTAL ELASTIC SPINE BRACED FRAMES

L. Chen[(1)], S. Pejmanfar[(2)], L. Tirca[(3)]

[(1)] *Assistant researcher, Concordia University Montreal, Canada, liang.chen@mail.concordia.ca*
[(2)] *Graduate student, Concordia University Montreal, Canada, s_pejman@encs.concordia.ca*
[(3)] *Associate professor, Concordia University Montreal, Canada, Lucia.Tirca@concordia.ca*

Abstract

The goal of this paper is to analyze the seismic performance of multi-storey braced frame buildings and to quantify the earthquake-induced losses and potential collapse risk of a newly developed structural system, labelled segmental elastic spine braced frame (SESBF), versus the eccentrically braced frame (EBF). The SESBF was derived from the conventional EBF with the aim of preventing the concentration of damage within one or a few floors of building studied when subjected to severe ground motions. The elastic spines of SESBF are the two trusses formed with beams outside of links, columns, braces and vertical ties. The full-height elastic spine is divided into a number of segments with the intent of minimizing the axial forces triggered in the truss members by the effects of higher vibration modes. From previous studies conducted on a 16-storey archetype building located in Vancouver, B.C., Canada, it resulted that SESBFs with two segments is a cost-effective system in mitigating damage concentration in the structure without introducing significant axial forces in the structural members. However, the typical design process was not performance-based, although the structural system response was verified through nonlinear time history analyses considering incremented levels of earthquake shaking. For comparison purpose, the archetype building is also designed with an EBF system to assess the improvements of the SESBF.

To quantify the earthquake-induced losses and assess the collapse risk (e.g. the collapse margin ration), metrics are available in the literature. Herein, the selected assessment procedure is intensity-based and the methodology employed is presented in FEMA P58 (2012). Consequently, the structural and nonstructural components of selected multi-storey building are categorized into fragility groups and performance groups. The fragility groups are made of similar components that have the same potential damage characteristics and the performance groups are part of a fragility group that experiences the same earthquake demands in response to earthquake shaking. The incremental dynamic analysis was conducted for each structure model subjected to earthquake records of different intensity levels. Results of the incremented dynamic analyses expressed in terms of interstorey drift, residual interstorey drift, link rotation, and floor acceleration are used to build fragility curves. With Performance Assessment Calculation Tool (PACT), hundreds of possible performance outcomes are realized, and the consequences of each damage level are then summarized as economic loss represented by the loss vulnerability curves (e.g. structural repair loss, nonstructural repair loss, demolition loss, collapse loss and total loss).

The innovative features of this study are as follows: the presentation of SESBF system's performance against the EBF system; the impact of modelling assumtions in the accuracy of results obtained using the OpenSees framework; the suitability of intensity-based performance assessment when earthquake-induced losses are computed as a tool to communicate performance.

Keywords: Probability of collapse, Earthquake-induced loss, Nonlinear response history analysis, Performance, Steel

1. Introduction

Building's seismic performance is deemed suitable when the seismic response shows an acceptable probability of collapse under the 2% in 50 years design-intensity earthquake [1]. Although a code-designed building could achieve the objective of preventing loss of life-threatening it may exhibit extensive damage transposed in economic loss. To communicate the performance of a building in ways that better relate to the decision-making needs, a next-generation of performance based seismic design (PBSD) was released in FEMA P-58-1 [2]. The framework, for the new released PBSD, is open to quantitative criteria that respond to stakeholders' decisions. After the quantitative criteria are defined, the type of performance assessment procedure is selected. To quantify the probable building performance for code design earthquake and other target intensity levels, the intensity-based assessment procedure can be used. The shaking intensity is defined by the elastic response spectrum. The flowchart of seismic performance methodology assessment provided in [2], presents the following steps: i) assemble building performance model, ii) define earthquake hazard, iii) analyze the building seismic response, iv) develop the collapse fragility curve and v) calculate performance.

The aforementioned methodology is applied to assess the seismic performance of an 8-storey building of normal importance category located in Victoria, British Columbia, Canada. Two seismic force resisting systems such as the eccentrically braced frame with short links, EBF (Fig. 1a) and segmental elastic spine braced frame, SESBF (Fig. 1e) were selected to brace the studied building.

It is known that the EBF system exhibits large ductility and high energy dissipation because of the wide and stable hysteresis response of its shear-yielding links. However, multi-storey EBFs are prone to seismic induced damage that may concentrate in only one or a few floors which impedes their performance and limit their capacity to redistribute inelastic demand in the non-yielding storeys [3]. Researchers tried to overcome this problem with additional members that run through the full height of the EBF to tie the links on all floors vertically. Such system is known as the Tied Braced Frame (TBF) [4] and is illustrated in Fig. 1b. The vertical ties, beam segments outside of links, columns and braces form a vertical elastic truss on each side of the links, which helps the frame to distribute the inelastic demand throughout the entire system. This concept of elastic truss(es), spine or strongback system has been used to improve the seismic response of structural systems such as Concentrically Brace Frame [5, 6] (Fig. 1c) and Buckling Restrained Braced Frame [7] (Fig. 1d). The TBF system demonstrated very stable seismic response at the cost of exponentially increasing force demand in the tie members. To reduce the force demands in the elastic trusses while maintaining the benefits of having vertical elastic spines in the system, an innovative Segmental Elastic Spine Braced Frame (SESBF) was proposed [8]. The yielding mechanism of an 8-storey two-segment SESBF is shown in Fig. 1e. A practical design approach was also developed [9]. The full height elastic truss is carefully divided into a series of connected smaller trusses based on a simple preliminary selection process [10]. The SESBF system can prevent damage concentration in EBFs with minimum added cost.

According to the performance methodology assessment, the structural and nonstructural components of selected building are categorized into fragility groups and performance groups. It is noted that fragility groups are made of similar components that have the same potential damage characteristics and performance groups are parts of a fragility group that experience the same earthquake demands in response to earthquake loading. The earthquake hazard is intensity-based and the selected analysis method is the nonlinear response history analysis. The selected engineering demand parameters are interstorey drift, link rotation, residual interstorey drift and floor acceleration. To assess the building performance, the modes of structural collapse are required in order to develop the adjusted collapse fragility functions. To calculate losses associated to the building seismic response, the Performance Assessment Calculation Tool (PACT) software [11] was employed and hundreds realizations were considered. Each realization represents one possible performance outcome. The suite of each performance outcome corresponding to a suite of earthquake intensity form the loss vulnerability curves such as: structural repair loss, nonstructural repair loss, demolition loss, collapse loss and total loss. In PACT, the replacement cost is used when the building exhibits a damage level that renders it irreparable. This occurs when the residual interstorey drifts exceed the level considered practicable to repair or when collapse occurs. The replacement cost includes replacement of building structure, exterior enclosure, the mechanical, electrical, and plumbing system, etc. The building is considered irreparable when 50% of replacement cost is required [2].

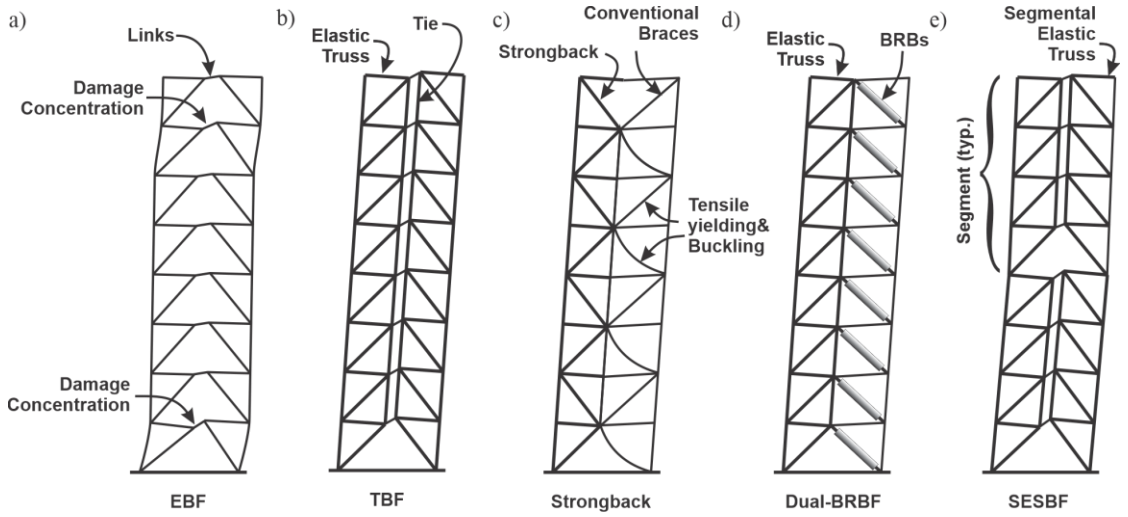

Fig. 1 – Framing system configurations

2. Building and Framing System studied

2.1 Basic Building Data and Fragility Performance groups

The case study is an 8-storey architype office building located on Site Class C in Victoria. The building is of normal importance category and the floor plan is shown in Fig. 2a. The lateral resistances along both orthogonal directions are provided by braced frames. As depicted, there are four braced frames displaced symmetrical in each direction. Due to building's symmetry, the calculation is conducted for one quarter of building's floor plan which includes one seismic force resisting system (SFRS) and ¼ of gravity columns that are laterally supported by the studied braced frame. The direction of calculation is E-W and the studied EBF and SESBF are plotted in Fig. 2b. For the 8-storey SESBF system, a two-segment configuration with 4-storey per segment was selected. All columns in the structure are continuous over two-storey. The gravity loads such as: dead load, live load, and snow load, as well as the cladding load are given in Fig. 2c. According to [2], the following designation is considered: N = the total number of vulnerable storeys of a building and the roof is always (N+1). As shown in Fig. 2b, floor level N comprises the slab at the level and all structural and nonstructural components up to the storey immediately above.

The structure design was performed in accordance with the provisions of National Building Code [12] and the Steel Design Standard [13]. The braced frames were designed to suffice both the capacity and deflection requirements when subjected to both seismic load and wind load. Link beams in EBFs can be selected between regular links that are part of roof and floor beams and replaceable links that are bolt connected to the beams [13]. In this study, replaceable links are considered to allow uniformly distributed overstrength ratio of ductile links while reducing the repair cost. The links were made of ASTM A992 W shapes with F_y = 345 MPa. The length of the links (e) was selected so that it would yield in shear while maintaining link plastic rotation within the code prescribed limit of 0.08 radians. According to capacity design principles, the links were designed first to resist the code specified seismic-induced forces. The remaining framing elements i.e. beam segments outside of links, columns, braces and ties, were designed based on the probable shear resistance of the shear-yielding links including strain-hardening effects and the associated gravity loads effects. Beams and columns were ASTM A992 W shapes, whereas braces and ties were ASTM A500 square tubes. As indicated, for columns, the same section was kept for two consecutive floors, which is common in practice. Using the equivalent static force procedure presented in [12], the seismic design base shear, V_{static}, is calculated as:

$$V = \frac{S(T_a)M_V I_E W}{R_d R_o} \quad (1)$$

where $S(T_a)$ is the spectrum acceleration at fundamental period of the structure, T_a, of the design spectrum, M_v is the higher mode effect on base shear, I_E is the importance factor, W is the seismic weight including 25% of snow load and R_dR_o are the ductility-related and overstrength-related force modification factors, respectively. The fundamental period can be calculated using the equation: $T_a = 0.05h_n$, where h_n is the total building height [12]. In this case study, h_n = 30.4 m and T_a = 1.52 s for both EBF and SESBF systems. The base shear, V, computed with Eq. (1) is 4668 kN, where R_d = 4, R_0= 1.5, I_E =1, M_V = 1, $S(T_a)$ = 0.27 g and W = 101437 kN. These characteristics are given in Table 1.

To simplify the design and fabrication process of SESBF system, all links displaced along a vertical truss segment height, which is 4-storey height in this case study, were considered identical and designed to carry the average shear force computed from the shear assigned to each link according to the spectral distribution pattern. The vertical ties were designed to carry the shear link capacity forces, while reducing the links rotation demands. The design of SESBF system is based on a dynamic procedure according to [9, 10].

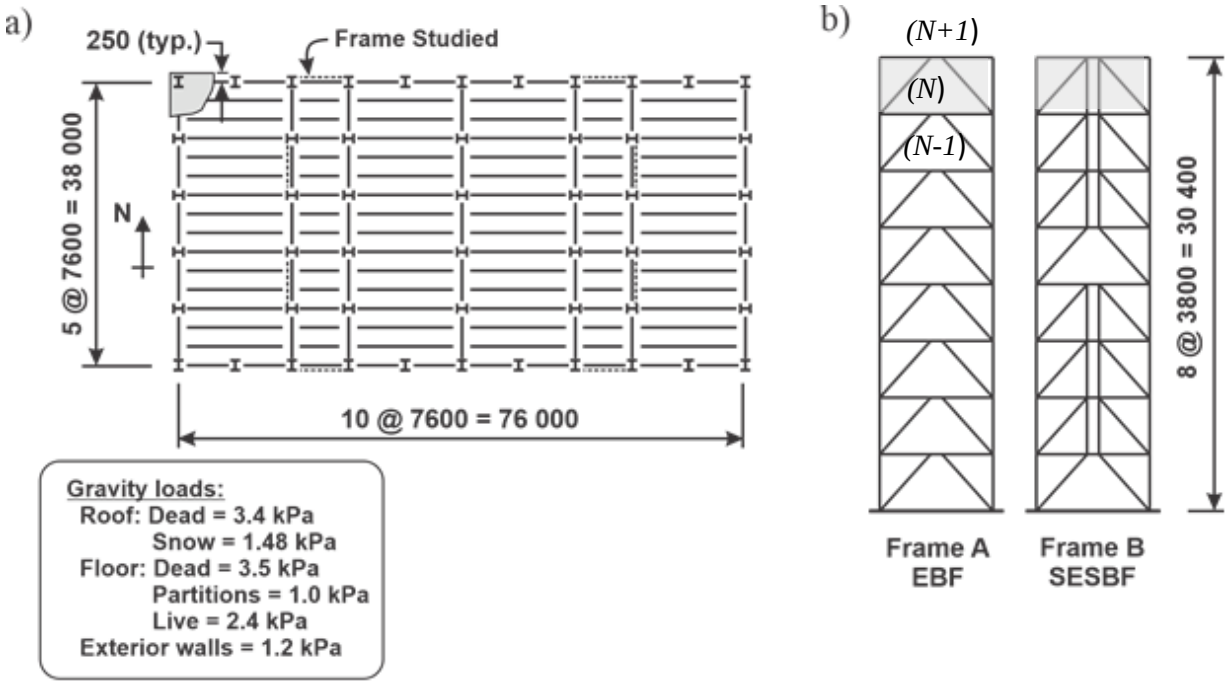

Fig. 2 – Building studied: a) Floor plan, b) Elevation of 8-storey framing systems, c) Loads

Table 1 – Structural properties of studied frames

Type	T_a	W	V_{static}/frame	T_1	T_2	T_3	$V_{dynamic}$/frame
	(s)	(kN)	(kN)	(s)	(s)	(s)	(kN)
EBF	1.52	101437	1167	2.27	0.77	0.42	933
SESBF	1.52	101437	1167	2.10	0.72	0.35	1080

2.1 Ground motions

For Victoria, seismic hazard is contributed mostly by shallow crustal earthquakes and subduction earthquakes. Ground motions are selected to reflect the magnitude-distance scenario. The spectral shape matching is also a good indicator for records selection. According to the current building code, 11 records per suite are deemed sufficient for analysis. In this study, 15 crustal records corresponding to Site Class C (360 m/s < $V_{S,30}$ < 760 m/s) in Victoria are considered and their seismic characteristics are provided in Table

2. Herein, $V_{S,30}$ is the average shear wave velocity in the top 30 m, the PGA and PGV are the peak ground acceleration and peak ground velocity, respectively, t_D is the Trifunac duration, Tp is the main period of ground motion record and Tm is the mean period. The procedure applied to scale the ground motions requires that the mean spectrum of the selected suite is above the design spectrum in the period range of $0.2T_1$ to $1.5T_1$, while the design spectrum is associated to 2% probability of exceedance in 50 years which corresponds to a rare earthquake with 2475 year return period. The 2% in 50 years spectra for Site Class C in Victoria is plotted in Fig. 3 together with the scaled records.

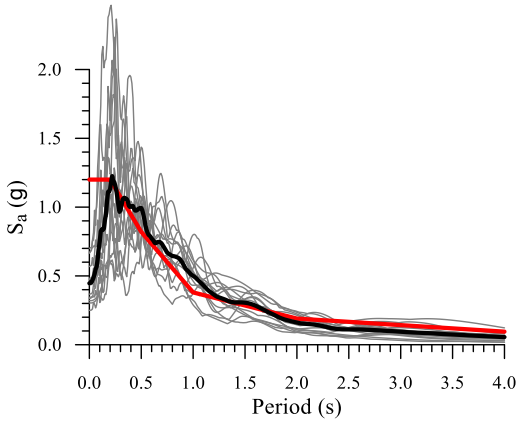

Fig. 2 – Spectrum of selected crustal ground motion records

Table 2 – Selected ground motion records and their seismic properties

No	NGA	Event	M_W	R_{hyp}	Com (◦)	PGA (g)	PGV (m/s)	t_D (s)	V_{s30} (m/s	SF	F.M EBF	F.M. SESB
1	953	Jan. 17, 1994 Northridge	6.7	22	9	0.42	0.59	9.21	365	0.6	3	II
2	963	Jan. 17, 1994 Northridge	6.7	44	90	0.57	0.52	9.08	450	0.7	3	I
3	986	Jan. 17, 1994 Northridge	6.7	25	195	0.19	0.24	11.43	417	1.8	2	I
4	1005	Jan. 17, 1994 Northridge	6.7	37	180	0.18	0.20	13.26	452	2.0	2	I
5	1006	Jan. 17, 1994 Northridge	6.7	25	90	0.28	0.22	11.30	398	1.7	1	I
6	1039	Jan. 17, 1994 Northridge	6.7	36	180	0.29	0.20	14.22	342	1.7	1	I
7	1049	Jan. 17, 1994 Northridge	6.7	25	280	0.20	0.15	10.45	360	2.0	1	I
8	57	Feb. 9, 1971 San Fernando	6.6	29	291	0.27	0.26	15.35	450	1.8	3	I
9	735	Oct. 18, 1989 Loma Prieta	6.9	65	0	0.16	0.16	14.68	415	2.0	2	I
10	767	Oct. 18, 1989 Loma Prieta	6.9	36	0	0.56	0.36	6.37	360	1.0	3	I
11	787	Oct. 18, 1989 Loma Prieta	6.9	54	360	0.28	0.29	11.58	425	1.3	1	I
12	796	Oct. 18, 1989 Loma Prieta	6.9	99	90	0.20	0.32	8.72	594	1.6	1	I
13	1787	Oct. 16, 1999 Hector Mines	7.1	30	90	0.34	0.42	9.66	726	1.0	1	I
14	1794	Oct. 16, 1999 Hector Mines	7.1	54	360	0.19	0.24	12.9	379	1.6	3	I
15	15	July 21, 1952 Kern County	7.4	46	21	0.16	0.15	30.30	385	2.2	3	I

3. Analysis and Results

3.1 Numerical models

The nonlinear response history analyses were carried out using the OpenSees platform [14]. The 2D model

was developed for one quarter of the building and includes one bracing bent acting in the E-W direction and ¼ of gravity columns that are laterally supported by the studied braced frame. The shear links were modelled using elastic beam-column elements with *zeroLength* elements at one end replicating the elastic bending and nonlinear shear responses of links [15]. *Steel02* material was assigned to the *zeroLength* element to mimic a shear spring that simulates the link hysteretic response including isotropic and kinematic strain hardening. In addition, *Min-Max* material was asigned in parallel to the *Steel02* material to account for fracture of links that occurs at maximum link rotation. The *Min-Max* material was calibrated against the results of experimental tests reported in [16] and according to their findings, an average link rotation of 0.108 radians occurs at failure instead of 0.08 radians as provided in [13]. The calibration of OpenSees model for links yielding in shear is presented in [8]. Although the vertical truss members of SESBFs are expected to behave elastically, all members were modelled using nonlinear beam-column elements with distributed plasticity and fiber cross-section discretization to detect potential yielding or buckling in the members. The *Steel02* material was assigned to these elements and an initial out-of-straightness was assigned to braces, columns and ties. The probable yield strength of steel material was considered as 385 MPa for I-shapes/W-shapes members and 460 MPa for HSS members. A 3% of critical damping assigned to structural members responding in the elastic range was specified with Rayleigh method in the first and third vibration mode. P-Δ effects were considered in the analyses with tributary gravity loads composed of dead load plus 50% of live load and 25% of roof snow. The gravity load was applied to the braced frame and leaning columns. Notional loads were also considered. To demonstrate the nonlinear behaviour of shear links, in Fig. 4, the response of the 7th storey's link of the EBF frame under the #953 ground motion scaled to 1.0x$S_a(T_1)$ is plotted, where $S_a(T_1)$ is the acceleration spectral ordinate at design level which is 0.17g.

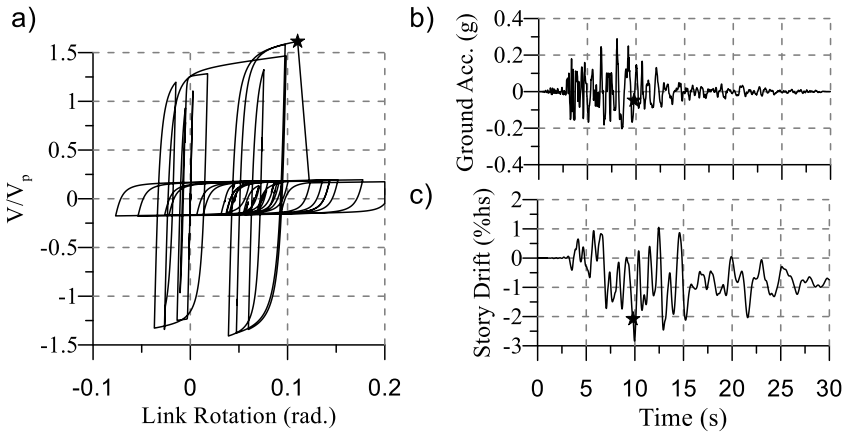

Fig. 4 Response of 7th floor's EBF under GM #953; a) link hysteresis, b) Scaled accelerogram, c) Storey drift

3.2 Design level

To assess the distribution of nonlinear seismic response along the building height, the recorded parameters were: interstorey drift, residual interstorey drift, link rotation and floor acceleration. In the case of EBF building, the spectral acceleration ordinate corresponding to T_1 = 2.27 s is $S_a(T_1)$ =0.17 g corresponding to design level. The first mode period of the SESBF building is T_1 = 2.1 s; hence, it is slightly shorter than that of EBF building. The associated spectral acceleration ordinate is $S_a(2.1)$ = 0.176 g. The interstorey drift, link rotation, residual interstorey drift and floor acceleration across the building's height were recorded at design level and are presented for both buildings in Figs. 5, and 6, respectively. The mean and mean + standard deviation (Mean+SD), computed for the seismic response parameters resulting from the suite of scaled ground motions are also plotted in these figures. As depicted in Fig. 5a, the peak of mean interstorey drift is within the code limit, which is 2.5%h_s. However, the Mean+SD of EBF shows large interstorey drift demand especially at the upper half floors where the links rotation exceeds 0.11radians under a few ground motions. The peak of mean residual interstorey drift is larger than 0.5 %h_s which means that building demolition may occur under earthquake events of design spectrum intensity. Thus, the 8-storey EBF building, designed in

high risk seismic zones, does not behave as expected. Comparing the interstorey drift configuration along the building's height for SESBF versus EBF, it appears that for a small increase of structural system cost, the response is significantly improved. For the SESBF building, the mean and Mean+SD of interstorey drift is around 1.0 %h_s and that of residual interstorey drift is below 0.5 %h_s. The mean of links rotation is about 0.05 radians and the Mean+SD is below 0.07 radians and the mean of floor acceleration is around 0.5 g. Clearly, under the crustal record suite, the seismic demand is uniformly distributed along the building height.

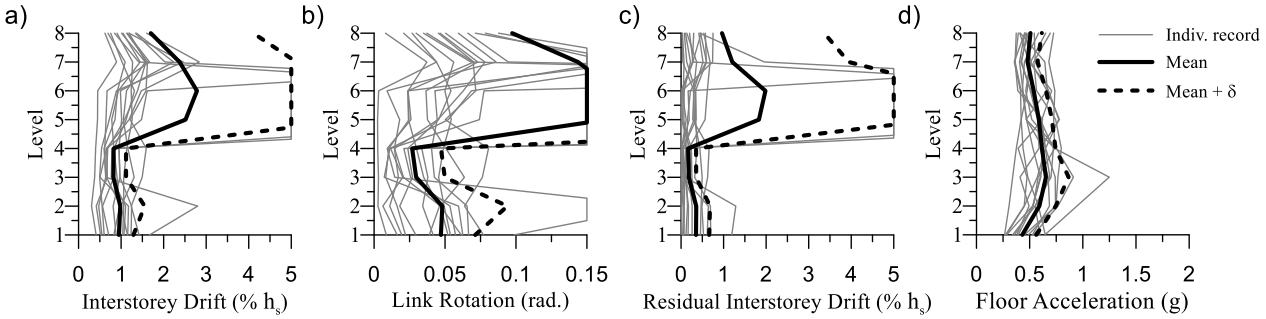

Fig. 5 - Seismic response at design level of EBF: a) interstorey drift, b) link rotation, c) residual interstorey drift, d) floor acceleration

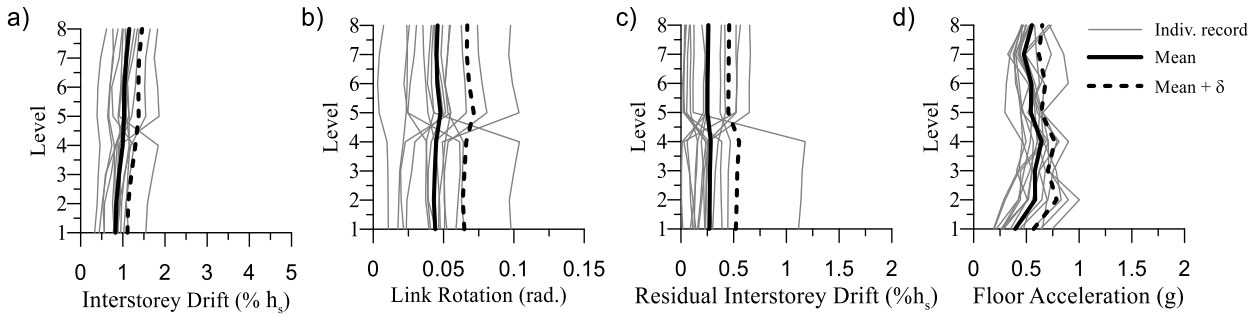

Fig. 6 - Seismic response at design level of SESBF: a) interstorey drift, b) link rotation, c) residual interstorey drift, d) floor acceleration

3.3 Incremental dynamic analysis

Incremental dynamic analysis (IDA) [17] is employed using the same suite of ground motions scaled to a series of incremented intensity levels considering a multiple of 0.05g. The selected intensity measure (IM) is the 5% damped spectral acceleration at the first-mode period of the building, $S_a(T_1,5\%)$.For the engineering demand parameter (EDP), the potential candidates are: interstorey drift, residual interstorey drift, link rotation and floor acceleration. To emphasize the most suitable EDP that expresses the response of EBF and SESBF buildings from yielding to failure, four IDAs sets are computed and depicted in Figs. 7 and 8, respectively. When IDA curves are expressed in terms of interstorey drift, the median IDA curve computed under the suite of 15 ground motions is shown in Fig. 7a and 8b for both EBF and SESBF. Thus, for the EBF, the median interstorey drift at failure is 1.67 %h_s under $S_a(T_1)$ = 0.17g, which is the design level. Conversely, the 50 percentile IDA for SESBF shows that the median interstorey drift at failure is 2.0 %h_s and is associated to $S_a(T_1)$ = 0.37g which is about two times the $S_a(T_1)$ at design level. As resulted, the capacity of SESBF to sustain earthquake-induced damage is greater than that of EBF.

Analyzing the IDA shapes, it results that the EBF system shows softening behaviour which means that damage accumulates at higher rates. Meanwhile, the IDA curves of SESBF show elastic response until the links within a segment exhibit shear–induced failure. As resulted, both structural systems are not prone to drift induced damage, as far as, the link does not exceed its rotation capacity of 0.11 radians. From Figs. 7b and 8b it results that the median link rotation at failure is 0.086 radians for EBF and 0.11 radians for SESBF, respectively. The median residual interstorey drift depicted in Figs. 7c and 8c is 0.59 %hs for EBF and 0.53 %hs for the SESBF. In Figs. 7d and 8d is shown that the median floor acceleration is 1.25 g for EBF and

1.02 g for SESBF, respectively. Both EBF and SESBF show similar median engineering demand parameters at failure, but the SESBF can sustain severe earthquake demand with lower probability of failure.

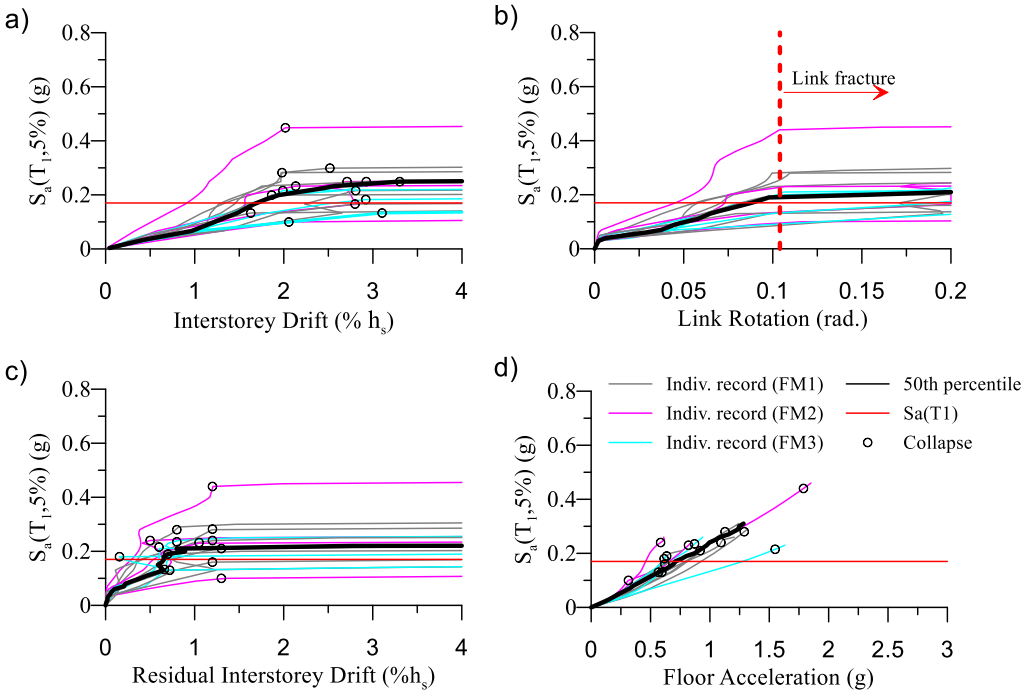

Fig. 7 - The IDAs of the EBF building expressed in terms of: a) interstorey drift, b) link rotation, c) residual interstorey drift and d) floor acceleration

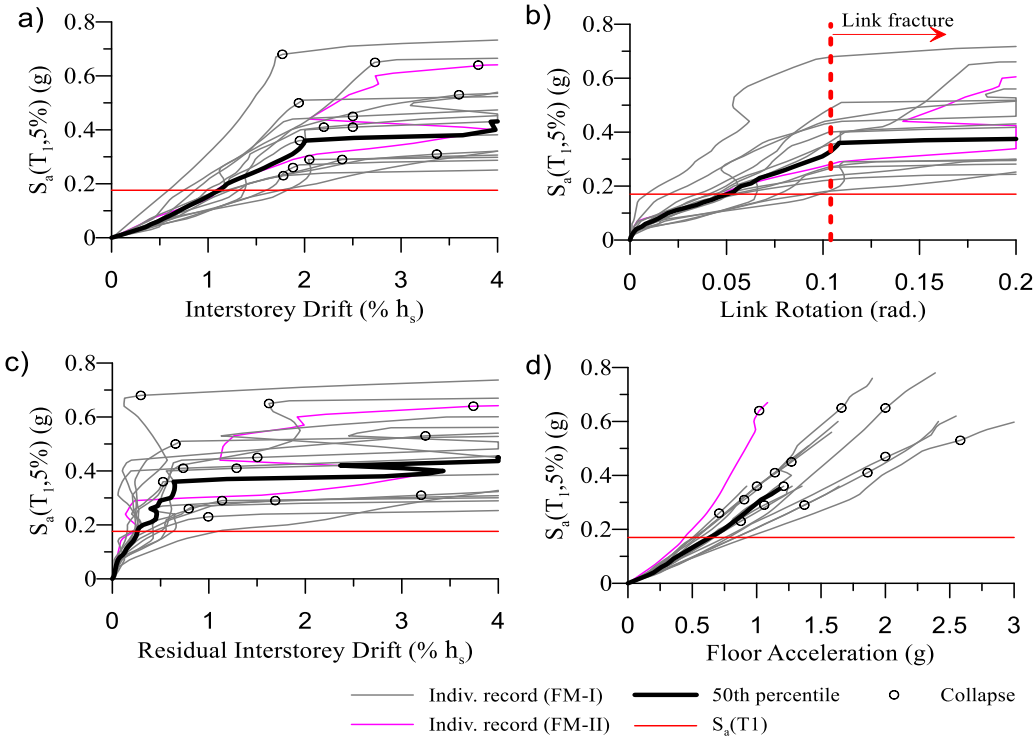

Fig. 8 - The IDAs of the SESBF building expressed in terms of: a) interstorey drift, b) link rotation, c) residual interstorey drift and d) floor acceleration

4. Assessment of Collapse Performance

To assess the collapse performance of studied 8-storey building, the methodology presented in FEMA P-695 [1] is applied. Consequently, the probability of collapse due to design earthquake ground motions (2%/50 years) should be limited to 10%. To verify this criterion, the collapse margin ration, CMR, should be computed. By definition, CMR $=\hat{S}_{CT}/S_a(T_1)_{design}$, where $\hat{S}_{CT}$ is the median collapse capacity defined at the intensity of ground motion at which half of the records in the selected suite cause collapse and $S_a(T_1)_{design}$ is the design spectral acceleration intensity at T_1. To account on uncertainties, the adjusted collapse margin ratio, ACMR, is considered and calculated as the product CMR *x SSF*, where *SSF* is the shape factor as per [1]. These parameters computed for both SFRSs are given in Table 3. Larger ACMR value shows that the studied SFRS possesses a larger margin safety to collapse. The lognormal standard deviation parameter β_{TOT}, describing the total collapse uncertainty is computed as: $\beta_{TOT} = (\beta_{RTR}^2 + \beta_{DR}^2 + \beta_{TD}^2 + \beta_{MDL}^2)^{0.5}$ where β_{RTR} = record-to-record collapse uncertainty, β_{DR} = design requirements-related collapse uncertainty, β_{TD} = test data-related collapse uncertainty and β_{MDL}= modeling-related collapse uncertainty. To quantify β_{TOT} according to [1] the following assumptions are made: (1) the quality of design requirements were considered as "(A) Superior" with corresponding β_{DR}=0.1; (2) the quality of test data was considered as "(B) Good" with corresponding β_{TD}=0.2; (3) the model quality was considered as "(B) Good" with corresponding β_{MDL}=0.2. From calculation it results β_{TOT} = 0.5. Acceptable values of adjusted collapse margin ratio are based on β_{TOT} and on the established values of acceptable probability of collapse based on the assumption that the distribution of spectral intensity at collapse is lognormal with a median value and a lognormal standard deviation equal to β_{TOT}. Figure 9 shows the adjusted collapse fragility curve which describes the probability of collapse P(C|IM) as a function of $S_a(T_1)$ for both EBF and SESBF systems. From Table 4 it results that EBF system fails to fulfill the collapse safety criterion. Moreover, the number of failure mechanism types and their percentage obtained under the suite of 15 ground motions were identified.

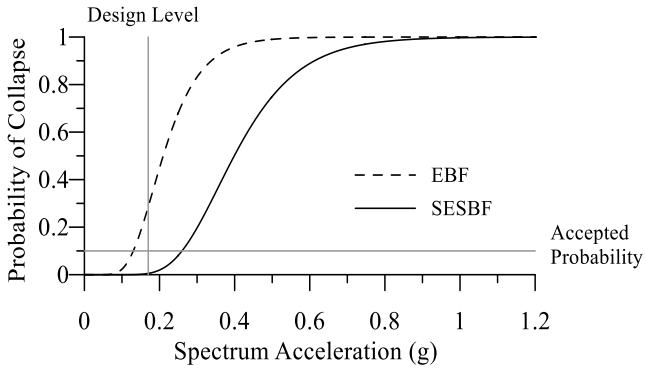

Fig. 9 - Adjusted collapse fragility curve of studied SFRSs

Table 4 – Evaluation of collapse safety of the studied SFRSs according to FEMA P695 methodology

Type	$S_a(T_1)_{design}$	$\hat{S}_{CT}$	CMR	ACMR	$ACMR_{10\%}$	ACMR/ $ACMR_{10\%}$	Pass/ Fail
EBF	0.170	0.17	1.0	1.4	1.9	0.74	Fail
SESBF	0.176	0.37	2.1	2.94	1.9	1.55	Pass

Analyzing the floors where links exhibited failure, three types of failure mechanisms were observed for EBF as per Fig. 10a and Table 2. Thus, 6 out of 15 ground motions (40%) caused links failure at bottom floors (FM1), 3 out of 15 ground motions (20%) caused links failure at 5th and 6th floors (FM2) and 40% of ground motions caused links failure at upper two floors followed then by bottom floors (FM3). It is worth mentioning that once the FM1 is developed, it triggers the building collapse. After the FM2 is developed, the upper half floors will exhibit collapse followed by building collapse. After the FM3 is developed and the upper floors reached failure, the links failure occur at bottom floors causing building collapse. The type of

failure mode of SESBF resulted under the 15 ground motions is different. Hence, as depicted in Fig. 10b, 93% of ground motions produced links failure within the bottom 4-storey segment (FM-I) and only 1 ground motion caused links failure within the top segment which was then followed by the lower segment (FM-II).

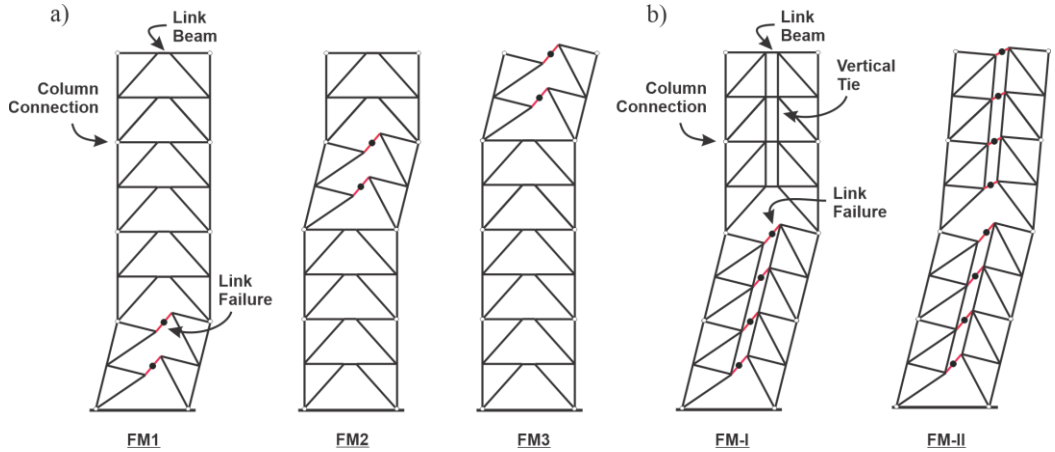

Fig. 10 - Failure modes: a) EBF system, b) SESBF system

4. Loss Assessment conditioned on seismic intensity

The building-specific loss estimation methodology discussed in [18], considers Eq. (2) to compute the total loss in a building (LT) subjected to an earthquake event with a ground motion intensity IM:

$$L_T = L_{NC\cap R} + L_{NC\cap D} + L_C \quad (2)$$

Herein, $L_{NC\cap R}$ is the loss in the building given that the collapse does not occur (no collapse) and the structure is repaired, $L_{NC\cap D}$ is the loss in the building where no collapse occurs but the building is demolished due to the significant cost associated with repairing and straightening the permanent deformations exhibited by structure and rebuilding is required, and L_C is the loss in the building when collapse occurs and the building shall be rebuilt. Assuming that these consequences are mutually exclusive, the expected value of the loss in the building for a given seismic intensity IM is computed as:

$$E[LT|IM]= E[LT|\ NC\cap R, IM]\ P(R|NC, IM)\ P(NC|IM)+E[LT|\ NC\cap D]\ P(D|NC, IM)\ P(NC|\ IM)+E[LT|C]\ P(C|IM)$$

where $E[LT|\ NC\cap R, IM]$ is the expected total loss in the building under an earthquake of intensity IM when collapse do not occur and reparation is required, $E[LT|\ NC\cap D]$ is the expected value of total loss in the building when there is no collapse but demolition is required. In the calculation, this loss is assumed to be equal to the replacement cost of the building plus additional 10% of replacement cost for demolition and site clearance. The E[LT|C] is the expected value of the total loss in the building when collapse occurs and this value corresponds to the replacement cost. Then, P(R|NC, IM) is the probability that the building will be repaired given that no collapse occurs and P(NC| IM) is the probability of no collapse for a given earthquake intensity IM. Furthermore, P(D|NC, IM) and P(C|IM) are the probability that the building will be demolished although no collapse occurs and the probability that collapse occurs, respectively, for the given earthquake intensity IM. Knowing the EDPs for a suite of intensity measure values at each floor and considering the fragility curves of nonstructural components provided in PACT library, a storey-based building specific loss estimation approach is employed.

Using data for an office building from RS Means [19], the total cost is $36.5 million and the building structure is 20% of total cost. Figures 11a and 11b present the loss-vulnerability curves for EBF and SESBF, respectively. Herein, the vertical line shows the economic loss in percentage of building replacement cost at various ground motion intensity levels expressed as $S_a(T_1)/S_a(T_1)_{design}$. In case of EBF, as depicted from IDA curves based on residual drift, for IM = 0.2 g, the residual drift increases more than 1.0 %h_s for 3 out of 15 ground motions and demolition is required. Furthermore, for IM = 0.28g, all ground motions but one caused

building's collapse. Conversely, for IM=0.28g, 4 ground motions out of 15 subjected the SESBF building to residual drift larger than 1.0 %h_s after links of bottom segment reached failure. At design-level intensity, minor damage of partition walls is expected for the SESBF. Alongside the plotted vulnerability curves, detailed distribution of damage exhibited by the drift-sensitive and acceleration-sensitive non-structural components is presented for incremented intensity levels in Figs. 11a and b. In terms of performance, it can be concluded that at design-level earthquake, the level of economic loss for EBF is about 50%, which is the threshold for building demolition and replacement. In case of SESBF, the 50% economic loss occurs for $S_a(T_1)/S_a(T_1)_{design}$=1.6. It is worth mentioning that PACT is correlated with RS Means and uses a highly repetitive Monte Carlo procedure to take into account the effect of a variety of uncertainties affecting the seismic performance. In the calculation, 100 realizations were considered to perform the seismic-induce loss calculations and each realization represents a possible seismic performance outcome. Herein, only the performance measure based on the repair cost was considered.

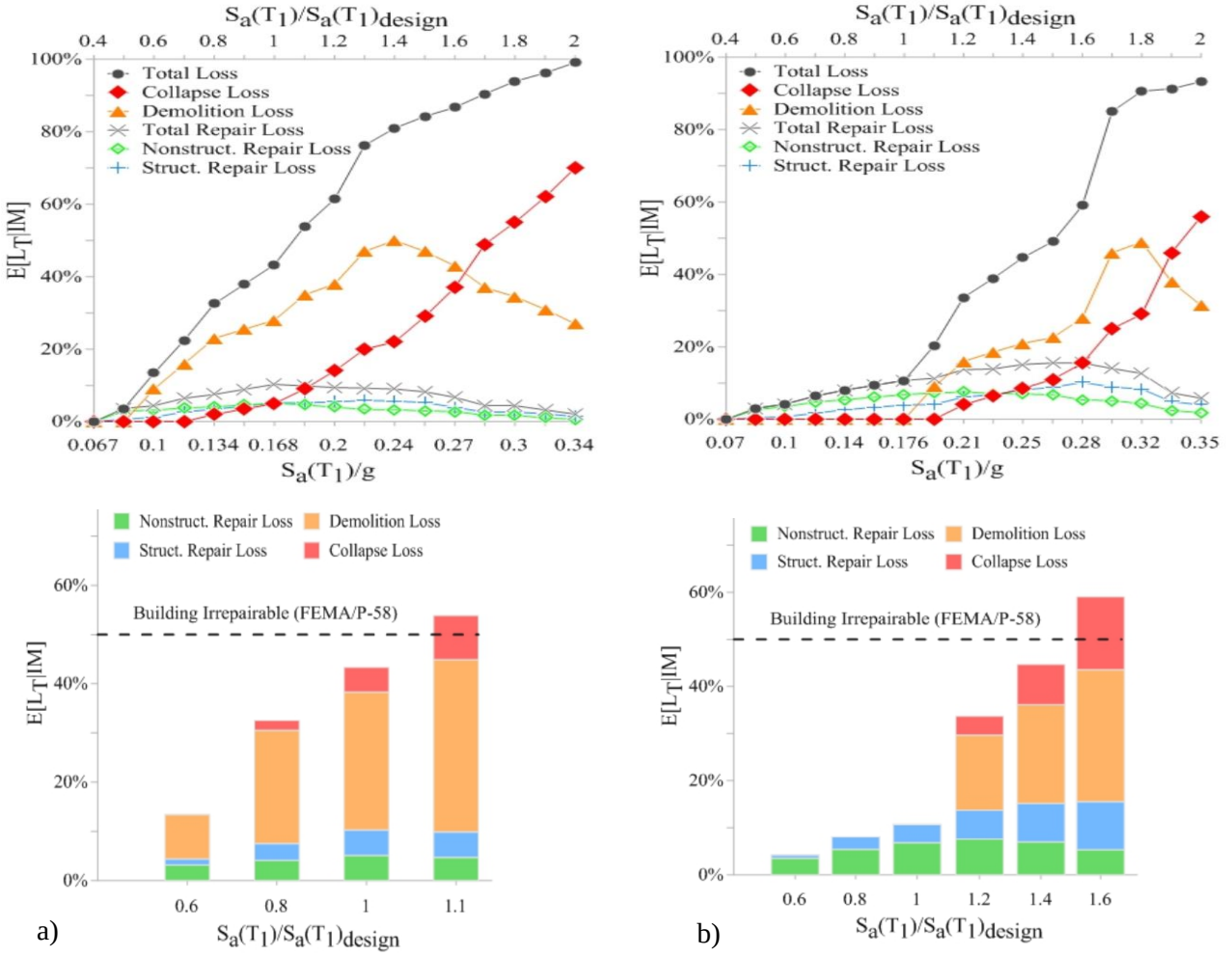

Fig. 11- Loss-vulnerability curves and distribution of % of losses at several IM levels: a) EBF, b) SESBF

5. Conclusions

The seismic performance of an 8-storey steel braced frame building located on firm soil in Victoria, B.C. is assessed using the intensity-based methodology linked to an earthquake-induced economic losses approach. Two SFRSs such as the EBF and newly developed SESBF were considered for performance evaluation. Thus, at 2% in 50 years design-level earthquake, the 8-storey EBF building experienced links failure at upper floors where large interstorey drifts were developed. Three types of failure mechanisms were identified under the suite of 15 crustal ground motions: FM1 - bottom two floors (40%), FM2 – the 5th and 6th floors

(20%) and FM3 - upper two floors followed then by bottom floors (40%). When FM1 or FM2 was generated, damage was concentrated within two floors that triggered building to collapse. Half of the records in the selected suite caused collapses at $S_a(T_1)_{design}$. In consequence, the EBF fails to pass the collapse safety criterion and caution should be given in design. Analyzing the loss-vulnerability curves, it was found that the level of economic loss is about 50% at 1.05 x design-level intensity which is the threshold for building demolition and replacement.

The 8-storey SESBF building showed a superior seismic performance than the EBF building. At 2% in 50 years design level earthquake, the SESBF is able to mitigate the interstorey drift (~ 1.0 %h_s) and shows an uniformly distribution along the building height. Conversely, the IDA curves of SESBFs show elastic response until the links within one segment exhibited shear failure. Two types of failure mechanisms were identified under the suite of 15 crustal ground motions: FM1 - bottom 4-storey segment (97%) and FM2 upper 4-storey segment followed by bottom segment (7%). In this case, the collapse margin ratio is 2.1 and the SESBF pass the collapse safety criteria and the ratio ACMR/$ACMR_{10\%}$ is 1.5. Thus, the 8-storey SESBF possesses sufficient reserve capacity and can be used in high risk seismic zones. Analyzing the loss-vulnerability curves its was found that the level of economic loss is about 50% at 1.50 x design-level intensity. The performance measure based on the repair cost was considered.

5. Acknowledgements

Financial support for this study from the Natural Sciences and Engineering Research Council of Canada and the Fonds de recherche Nature et technologies du Quebec (FRQNT) is gratefully acknowledged.

6. References

[1] FEMA (2009): Quantification of building seismic performance factors, FEMA P695, Washington.
[2] FEMA (2012): Seismic Performance Assessment of Buildings, FEMA P58-1, Washington.
[3] Ricles JM, Popov EP (1987): Dynamic analysis of seismically resistant eccentrically braced frames. Report No. ERCC 87-07, Earthquake Engineering Research Center, Univ. of California at Berkeley, Berkeley, CA.
[4] Rossi PP (2007): A design procedure for tied braced frames. *Earth. Eng. and Struct. Dynamics*, (**36):** 2227–2248.
[5] Lai JW, Mahin SA (2015): Strongback system: A way to reduce damage concentration in Steel-Braced Frames. *J. Struct. Eng.*, ASCE, **141**(9), DOI: 10.1061/(ASCE)ST.1943-541X.0001198.
[6] Simpson BG, Mahin SA (2018): Experimental and numerical investigation of Strongback Braced Frame system to mitigate weak story behavior. *J. Struct. Eng.*, **144**(2), DOI: 10.1061/(ASCE) ST.1943-541X.0001960.
[7] Tremblay R, Poncet L (2007): Improving the seismic stability of Concentrically Braced Steel Frames. *Eng. J.*, **44**(2), 103-116.
[8] Chen L, Tremblay R, Tirca L (2019): Modular tied eccentrically braced frames for improved seismic response of tall buildings. *Journal of Constructional Steel Research*, Vol. **155**, pp. 370-384.
[9] Chen L, Tremblay R, Tirca L (2019): Practical seismic design procedure for steel braced frames with segmental elastic spines. *Journal of Constructional Steel Research*, Vol. **153**, pp. 395-415.
[10] Chen L, Tremblay R, Tirca L (2019): Determination of optimum configurations for steel braced frames with segmental elastic spines. *Journal of Structural Engineering* (ASCE) DOI:10.1061/(ASCE)ST.1943-541X.0002398.
[11] FEMA (2012): Seismic Performance Assessment of Buildings, FEMA P58-2 (PACT), Washington.
[12] National Research Council of Canada (2010): National Building Code of Canada (NBCC), Ottawa, Canada.
[13] Canadian Standards Association (CSA) (2014): Design of steel structures, S16-14 Standard, Toronto, Ontario.
[14] OpenSees version 3.0.3(2019): Computer software, Berkeley, CA, Pacific Earthquake Eng. Research Center.
[15] Koboevic S, Rozon J, Tremblay R (2012): Seismic performance of low-to-moderate height eccentrically braced steel frames designed for North-American seismic conditions. *J. Struct. Eng.*, **138**(12), 1465-1476.
[16] Okazaki T, Engelhardt MD (2006): Cyclic loading behaviour of EBF links constructed of ASTM A992 Steel, *Journal of Construction Steel Research*, **63**, 751-765.
[17] Vamvatsikos D, Cornell C (2002): Incremental Dynamic Analysis, *Earth. Eng. & Struct. Dyn.*, **31**(3), 491-514.
[18] Ramirez CM, Miranda E (2012): Significance of residual drifts in building earthquake loss estimation, *Earthquake Eng. & Struct. Dynamics*, **41**(11): 1477-1493.
[19] RS Means Corporation, (2019): RS Means Square Foot Costs, Catalog No. 60054.

